Pergamon

Cement and Concrete Research 32 (2002) 1559–1565

CEMENT AND CONCRETE RESEARCH

Approximate migration coefficient of interfacial transition zone and the effect of aggregate content on the migration coefficient of mortar

C.C. Yang*, J.K. Su

Institute of Materials Engineering, National Taiwan Ocean University, Keelung 202, Taiwan

Received 4 January 2002; accepted 15 April 2002

Abstract

In this study, the electrochemical technique is applied to accelerate chloride ion migration in mortar to estimate its transport properties. In order to investigate the effect of aggregate content on the chloride migration coefficient of mortar, specimens with different fine aggregate volume fractions were cast and tested. The chloride migration coefficient of mortar was determined experimentally as a function of the volume fraction of aggregate. The chloride migration coefficient of mortar is used to assess the dilution, tortuosity and interfacial transition zone (ITZ) effects of aggregate in the cement-based composites. A model modified from the Bruggeman theory for the migration coefficient of mortar is used, and the regression analysis is used to determine the approximate chloride migration coefficient of ITZ. Based on the experimental and regression analytical results, the approximate ITZ migration coefficient is 2.83, 1.76 and 1.55 times of the matrix migration coefficient for the ITZ with the thickness of 20, 40 and 50 μm, respectively.
© 2002 Elsevier Science Ltd. All rights reserved.

Keywords: Migration; Transport properties; ITZ; Aggregate content

1. Introduction

The resistance to chloride ion penetration into concrete is a crucial parameter affecting the durability of reinforced concrete structures exposed to marine environment. Since the conventional chloride diffusion test for cement-based materials is time-consuming, the accelerated chloride ion diffusion test method was developed. The accelerated testing method has been used to evaluate the influence of pore size [1], the degree of hydration [2] and aggregate fraction [3].

Concrete permeability is controlled by the permeability of its constituent materials and their geometric arrangement. Shah [4] and Delagrave et al. [5] pointed out that the inclusion of aggregates in the hydrated cement past matrix has two opposite effects on the transport properties. The dilution and tortuosity effects reduce concrete permeability, while the interface transition zone (ITZ) and percolation effects increase permeability.

In normal concrete or mortar, the hydrated matrix surrounding the aggregate has different microstructures resulting from the water/cement ratio gradient developed at the interfacial layer [6]. This layer around the aggregate is called the ITZ, which is characterized by a higher concentration of calcium hydroxide crystals and an increased porosity relative to the matrix paste [7–11]. Many researchers have analyzed the microstructure of ITZ in cement-based materials by use of scanning electron microscopy (SEM) [12–15], energy-dispersion X-ray spectrometry (EDX) [16] and backscattered electron (BSE) imaging [17]. The porosity of the ITZ was measured by mercury intrusion porosimetry (MIP) [18]. The ITZ thickness is usually reported as a region between 30 and 50 μm [10,19,20], and the maximum porosity of ITZ is about three times higher than the matrix paste [21]. Researchers at National Institute of Standards and Technology (NIST) have developed numerical models to describe the microstructure of cement-based materials using digital image analysis techniques [22,23]. The models have applied to determine material properties [24] and electrical conductivity of ITZ [21,25,26]. Using a hard core/soft shell computer model, Winslow et al. [20] investigated the percolation characteristics of cement-based materials ITZ. Using the results of Winslow et al. [20], Shane et al. [21] pointed out that the ITZ has become percolated between the

* Corresponding author. Fax: +886-2-2462-5324.
E-mail address: ccyang@mail.ntou.edu.tw (C.C. Yang).

0008-8846/02/$ – see front matter © 2002 Elsevier Science Ltd. All rights reserved.
PII: S0008-8846(02)00832-3

Table 1
Mix design, volume fraction of aggregate and compressive strength

	Matrix, unit content (kg/m^3)					Aggregate		f_c'
Mix	Water	Cement	Slag	Fly ash	SP	Sand (kg/m^3)	V_f	(12-month) (MPa)
M0	482.4	746.0	348.1	149.2	14.9	0.0	0	47.51
M1	433.2	669.9	312.6	134.0	13.4	265.0	0.1	53.47
M2	384.0	593.8	277.1	118.8	11.9	530.0	0.2	60.89
M3	334.7	517.7	241.6	103.5	10.4	795.0	0.3	63.00
M4	285.5	441.5	206.0	88.3	8.8	1060.0	0.4	64.77

sand volume fractions of 0.45 and 0.49. Garboczi and Bentz [27] pointed out that the ITZ is modeled as a uniform property region of some conductivity, this conductivity depends on what thickness is chosen to represent the actual porosity gradient.

The chloride migration coefficient of mortars was obtained by using the accelerated chloride migration test (ACMT), and the migration coefficient was used to assess the effects of aggregate in the cement-based materials. In this study, mortar is considered as a composite material in which sand particles are embedded in a matrix of hardened cement paste, and the ITZ is around the sand particles. A model from the Bruggeman theory [28] was modified for the migration coefficient of mortar, and the regression analysis is used to determine the approximate chloride migration coefficient of ITZ.

2. Experimental program

2.1. Materials

Mortar is a cement-based composite in which aggregates are embedded in a matrix of cementitious paste. In this study, matrixes were made of ASTM Type I Portland cement, water, superplasticizer, slag and fly ash. In order to study the effect of aggregate on the chloride migration coefficient of mortar, different fine aggregate volume fractions of mortar (V_f, the volume of aggregate/the volume of mortar), ranging from 0% to 40%, were selected in the mix proportions. The mix proportions are shown in Table 1. For all mixes, the water/binder ratio was 0.4 and the dosage of superplasticizer was adjusted to obtain the required slump and slump flow. The densities of the constituent materials are listed in Table 2, and the grading of fine aggregate is summarized in Table 3.

Table 2
Densities of the constituent materials (g/cm^3)

Water	SP	Cement	Slag	Fly ash	Sand
1.00	1.20	3.15	2.20	1.66	2.62

Table 3
Grading of fine aggregate

ASTM sieve designation	Sieve size (mm)	Amount retained (%)
No. 4	4.75	0.35
No. 8	2.36	8.01
No. 16	1.18	23.51
No. 30	0.60	27.81
No. 50	0.30	28.95
No. 100	0.15	8.54
Pat		2.83

2.2. Specimen preparation

For each mix, a number of cylindrical specimens (ϕ 100 × 200 mm) were cast and cured. After demolding, the specimens were cured in water (23 °C) for 12 months. The compressive strength of specimens, obtained according to ASTM C 39-01, is listed in Table 3. The ACMT specimen (50 mm in thickness) was obtained by sawing the mid-portion of cylindrical specimen. Before the test, ACMT specimens were prepared following the specification in ASTM C1202-97. The lateral surface of specimen was coated with epoxy and the specimen was placed in the vacuum desiccator, the pressure <1 mm Hg (133 MPa) was maintained for 3 h. De-aerated water was added to immerse the specimen and the vacuum level was maintained for one additional hour. Specimen was soaked in the added water for 18 h after turning off the pump. Then the specimen was removed from water and placed in the ACMT setup.

2.3. ACMT

To perform the ACMT, a two-compartment cell [29], as shown schematically in Fig. 1, was used. It was developed to measure the cumulative chloride ions passing through the test specimen. The specimen was placed between two acrylic cells. Two mesh electrodes (10 cm diameter, #20 mesh brass screen) were placed on two sides of the specimen in such a way that the electrical field is applied primarily across the test specimen. One of the cells was filled with 0.30 N NaOH

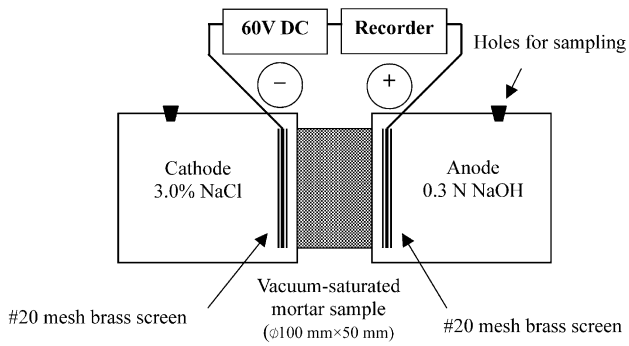

Fig. 1. Schematic diagram of accelerated chloride migration test cell.

solution and the other cell was with 3.0% NaCl solution. The cells were connected to a 12-V/cm (DC 60 V) power source in which the NaOH electrode becomes the anode and the NaCl electrode becomes the cathode. During the test, the chloride ion concentration was determined from the solution in the anode cell, titrated with 0.01N $AgNO_3$ standard solution by the potentiometric titration method in accordance with AASHTO T260-97.

3. Results and discussion

3.1. Migration coefficient

In the ACMT, chloride ions are transported in concrete under an applied voltage. As the chloride flux becomes constant, the general equation that describes transport processes in solution is the Nernst–Planck's equation [30]. In this equation, the total ion flux in the downstream cell J (mol/m^2/s) is made up of three components, namely diffusion, migration and convection, expressed as:

$$J = -D_i \frac{\partial C_i}{\partial x} - \frac{zF}{RT} D_i C_i \frac{\partial V}{\partial x} + C_i u \quad (1)$$

where D_i is the diffusion coefficient of ion i (m^2/s), which is later defined as a migration coefficient of mortar; T is the concentration of ion i (mol/m^3); R is the universal gas constant (8.3 J/mol/K); T is absolute temperature (K); V/x is the strength of the electric field between the anode and cathode (V/m); and u is the velocity of solute (m/s). The first and the third terms of Eq. (1) are the contribution due to diffusion and convection, respectively. Since the mortar is saturated, the velocity of solute can be neglected. Under the influence of an electrical field across the sample, the contribution of diffusion in concrete is small and can be neglected [30]. Only the second term is of paramount importance in the ACMT process and Eq. (1) is reduced to:

$$J = -\frac{zF}{RT} D_i C_i \frac{\partial V}{\partial x}, \quad (2)$$

and then the migration coefficient of chloride ions for mortar, D_{cl}, is calculated as:

$$D_{cl} = \frac{RT}{CF\left(\frac{V}{l}\right)} J_{cl} \quad (3)$$

where J_{cl} is the constant flux of chloride in the downstream cell (mol/m^2/s), C is chloride concentration in the upstream cell at the cathode and V/l is the electrical field (V/m).

The cumulative chloride ion concentration in the anode cell was measured periodically. The cumulative chloride ion concentrations versus time curves shown in Fig. 2 become quite linear after the chloride flux reached steady state. Linear regression is carried out to obtain the chloride ion migration rate, K, which is the slope of the cumulative chloride ion concentration versus time curve. The chloride flux (J_{cl}) in the anodic cell was calculated from the chloride ion migration rate and the chloride migration coefficient (D_{cl}) was calculated from Eq. (3). Both the chloride flux and the chloride migration coefficient are listed in Table 4. It appears that addition of fine aggregate to cement paste matrix enhanced the resistance of the mixture to chloride penetration.

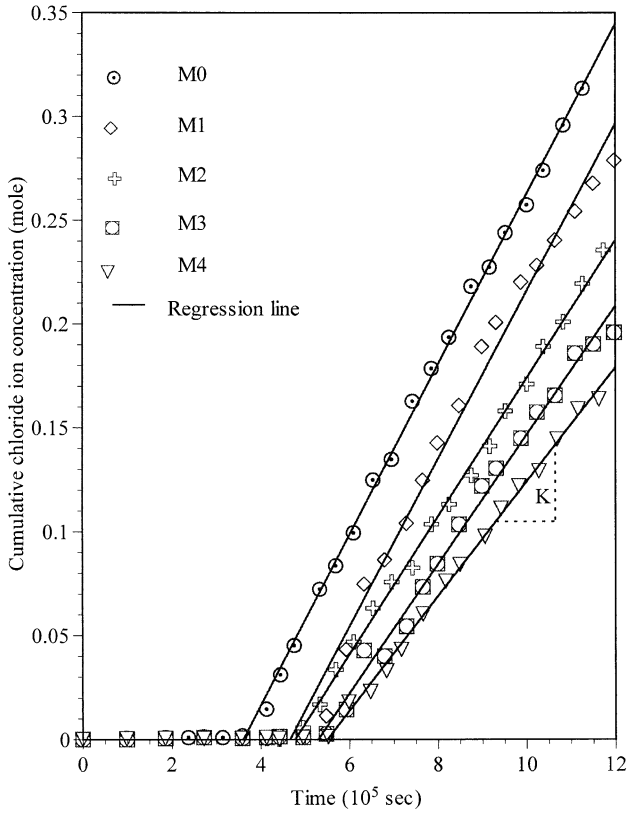

Fig. 2. Variations of cumulative chloride concentration in anode cell.

3.2. Effect of the aggregate on the chloride migration coefficient

Considering the aggregate is relatively impermeable, the chloride ion migration coefficient of mortar (D_{cl}) is controlled by the aggregate volume fraction and migration rate of paste. The chloride migration coefficient on a unit volume of paste ($D_p = D_{cl}/(1 - V_f)$) is computed and also listed in Table 4. The chloride migration coefficient on a unit volume of paste (D_p) increases with fine aggregate volume fraction. Delagrave et al. [5] pointed out that the increase of transport property on a unit volume of matrix is attributed to the porous ITZ between the paste and aggregate. Shah [4] proposed that the influence of aggregate in the hydrated cement past is fourfold: dilution, tortuosity, ITZ and percolation. In the previous study [29], the chloride ion migration rate of one series of mixture (C7) was measured and the same paste was used as in the present study. But, the volume fraction of total aggregate was 0.61 (fine aggregate volume fraction = 0.32, coarse aggregate volume fraction = 0.29). The chloride ion migration rate of Mix C7

Table 4
Results of the chloride flux, the chloride migration coefficient and migration coefficient on a unit volume of paste

Mix		Chloride flux J_{cl} (10^{-9} mol s^{-1}/cm^2)		Migration coefficient D_{cl} (10^{-8} cm^2/s)		$D_p = D_{cl}/(1 - V_f)$ (10^{-8} cm^2/s)	
			r^2		Average		Average
M0	M0-1	4.876	0.983	1.871	2.030	1.871	2.030
	M0-2	5.712	0.996	2.191		2.191	
	M0-3	5.288	0.938	2.029		2.029	
M1	M1-1	4.790	0.982	1.838	1.807	2.042	2.008
	M1-2	4.823	0.989	1.851		2.056	
	M1-3	4.518	0.986	1.733		1.926	
M2	M2-1	4.320	0.991	1.657	1.649	2.071	2.062
	M2-2	4.312	0.991	1.655		2.068	
	M2-3	4.266	0.975	1.637		2.046	
M3	M3-1	4.020	0.990	1.543	1.519	2.204	2.170
	M3-2	3.981	0.958	1.527		2.182	
	M3-3	3.875	0.998	1.487		2.124	
M4	M4-1	3.324	0.969	1.275	1.336	2.125	2.227
	M4-2	3.563	0.994	1.367		2.278	
	M4-3	3.563	0.996	1.367		2.278	

was 10.80 mmol/l/day. Comparing the chloride ion migration rates of Mix C7 (10.80 mmol/l/day), Mix M4 (0.99 mmol/l/day) and Mix M0 (7.98 mmol/l/day), Mix C7 is higher than Mix M4 and even much higher than Mix M0 (paste). The results indicate that the chloride ion migration rate in the present study was little affected by the percolation, because the specimens were cured in water for 12 months and the ITZs were not connected in the low aggregate volume fraction ($V_f = 0.1–0.4$) [21].

3.2.1. Dilution effect and tortuosity effect

Considering the aggregate is relatively impermeable and a linear parallel chloride ion flow exists. For the dilution effect, the migration coefficient of mortar, D_{cl}, can be expressed as [31]:

$$D_{cl} = D_o(1 - V_f), \tag{4}$$

where D_o is the migration coefficient of matrix and V_f is aggregate volume fraction. Combining the tortuosity effect with the dilution effect, the migration coefficient of mortar can be expressed by the Bruggeman equation [28]:

$$D_{cl} = D_o(1 - V_f)^{3/2}. \tag{5}$$

This model assumes that the migration coefficient of the matrix is constant as the spherical particles are added. In Fig. 3, the chloride migration coefficient of mortar is plotted as a function of the volume fraction of fine aggregate and are compared with the calculated results from Eqs. (4) and (5). It appears that the chloride migration coefficient decreases with an increase in fine aggregate volume fraction. The dilution and tortuosity effects reduce mortar permeability. At $V_f = 0.3$, when only the dilution effect is considered, the migration coefficient reduces from 2.03×10^{-8} to 1.42×10^{-8} cm^2/s. When combining the tortuosity effect with the dilution effect, the chloride migration coefficient reduces from 2.03×10^{-8} to 1.19×10^{-8} cm^2/s.

3.2.2. ITZ effect

The ITZ effect increases the chloride migration coefficient of mortar, as can be seen in Fig. 3. At V_f, the chloride migration coefficient is increased from 1.19×10^{-8} to 1.52×10^{-8} cm^2/s by ITZ effect. It can be seen from Fig. 3

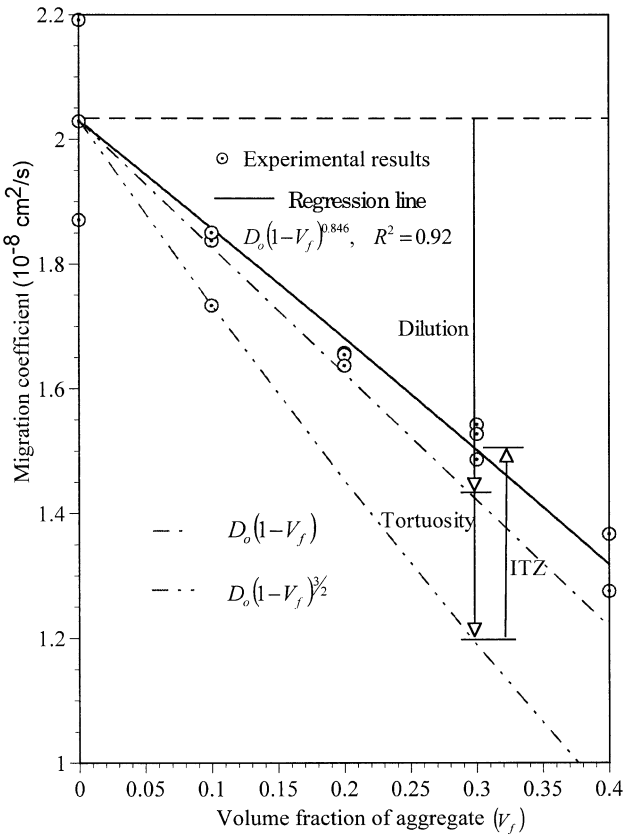

Fig. 3. Chloride migration coefficient versus volume fraction of aggregate.

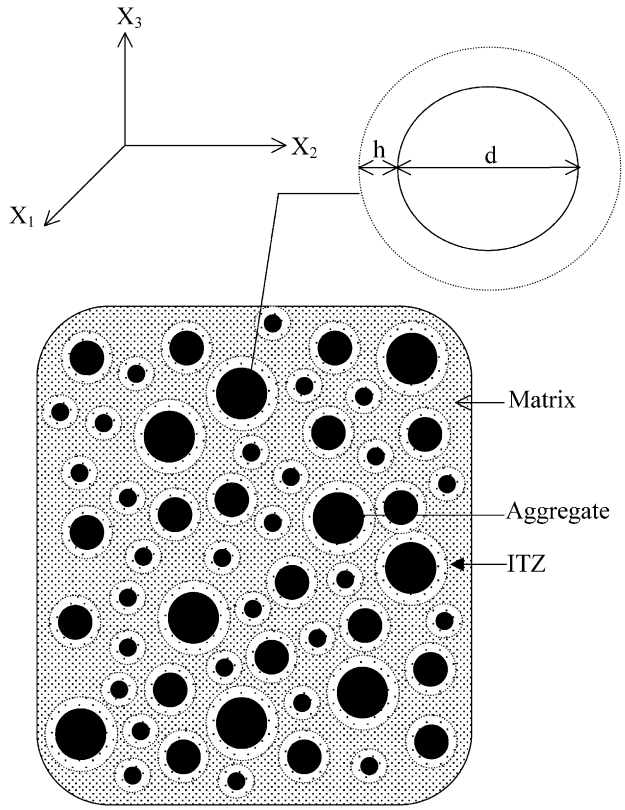

Fig. 4. Aggregate are modeled as spherical shape and ITZ as a layer around the aggregate which embedded in matrix.

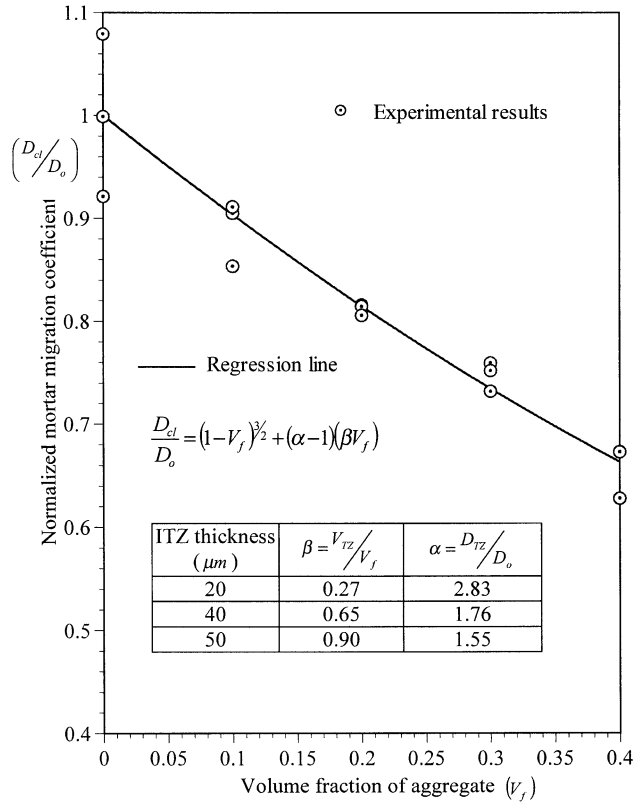

ITZ thickness (μm)	$\beta = V_{ITZ}/V_f$	$\alpha = D_{ITZ}/D_o$
20	0.27	2.83
40	0.65	1.76
50	0.90	1.55

Fig. 5. Experimental chloride migration coefficient of mortar normalized by chloride migration of paste versus aggregate volume fraction, and regression analytical results.

that the test data were above the theoretical results obtained from Eqs. (4) (dilution effect) and (5) (tortuosity effect and dilution effect). It is found that the chloride migration coefficient of mortar is affected by the ITZ, which develops between the aggregate and matrix paste. Therefore, it is reasonable to model the mortar as three-phase composites (matrix, aggregate and ITZ), and to consider the influence of aggregate in the hydrated cement past is dilution, tortuosity and ITZ in this study.

3.3. Approximate migration coefficient of ITZ

In order to investigate the approximate chloride migration coefficient of ITZ, the ITZ is considered as a uniform layer around the spherical shape of fine aggregate and the aggregate with ITZ is not overlapped (see Fig. 4). Combining the ITZ effect with the dilution and tortuosity effects, the migration coefficient of mortar can be expressed as:

$$D_{\mathrm{cl}} = D_{\mathrm{o}}(1 - V_{\mathrm{f}})^{3/2} + D_{\mathrm{o}}(\alpha - 1)(\beta V_{\mathrm{f}}), \tag{6}$$

where αD_{o} and βV_{f} are the migration coefficient of ITZ and the volume fraction of ITZ, respectively. This model assumes that the migration coefficient of the ITZ is constant and the chloride flow in the ITZ is locally parallel to the aggregate surface. In the ITZ, the chloride migration coefficient of matrix paste (D_{o}) is replaced by the chloride migration coefficient of ITZ (αD_{o}).

Table 5
Average size of aggregate and the value of β for different thickness of ITZ

			β (ITZ vol. fraction/aggregate vol. fraction) (10^{-5})		
Sieve size (mm)	Amount retained (%)	Aggregate average size, d (mm)	$h = 20$ μm	$h = 40$ μm	$h = 50$ μm
9.50	0.00				
4.75	0.35	7.13	6	12	15
2.36	8.01	3.56	273	552	694
1.18	23.51	1.77	1630	3334	4214
0.60	27.81	0.89	3921	8194	10,467
0.30	28.95	0.45	8427	18,348	23,907
0.15	8.54	0.23	5412	12,732	17,197
Pat	2.83	0.08	7372	22,150	33,122
Σ			27,041	65,322	89,615

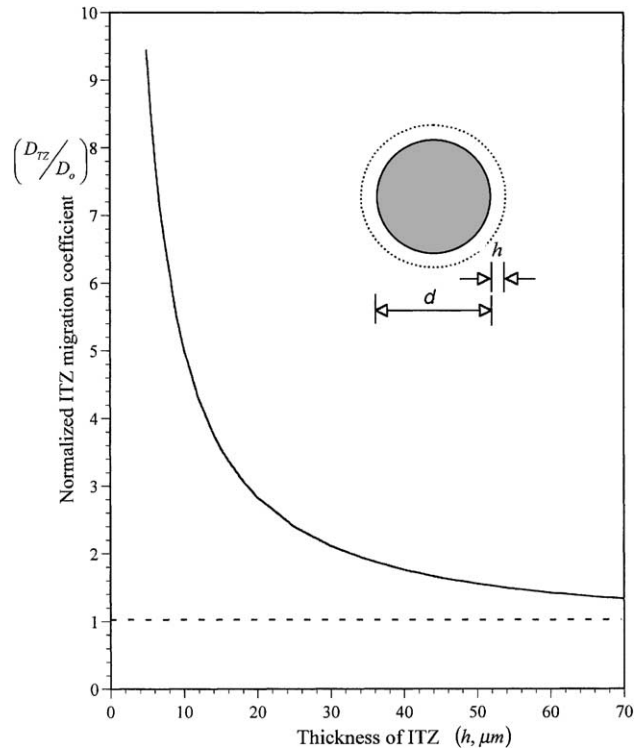

Fig. 6. Model chloride migration coefficient of interfacial transition zone normalized by chloride migration coefficient of matrix versus the thickness of interfacial transition zone.

When the thickness of ITZ (h) is assumed and the sieve analysis is used, the volume fraction of ITZ (V_{TZ}, the volume of ITZ/the volume of mortar) can be expressed as:

$$V_{TZ} = \beta V_f = V_f \sum \frac{R_i}{d_i^3}\left[(d_i + h)^3 - d_i^3\right] \quad (7)$$

in which R is individual retained ratio on i sieve and d is the average size of fine aggregate which restrained on i sieve. The thickness of ITZ is usually selected as a region between 30 and 50 μm [10,19,20]. When the thickness of ITZ (h) is assumed to be 20, 40 and 50 μm, the value of β is calculated from Eq. (7). The average size of fine aggregate that individual retained on each sieve and the value of β for different thickness of ITZ (20, 40 and 50 μm) are listed in Table 5.

Because it is difficult to test the ITZ separately, little information is available for the chloride migration coefficient of ITZ. For computing the approximate chloride migration coefficient of ITZ with the thickness of 20, 40 and 50 μm, the volume fraction of ITZ was calculated from Eq. (7) (see Table 5). Using regression analysis and the value of β from Eq. (7) (see Table 5), the approximate chloride migration coefficient of ITZ can be obtained from Eq. (6). Fig. 5 shows the relationship between normalized chloride migration coefficient of mortar and the aggregate volume fraction, and the corresponding regression results are also shown in this figure. Based on the experimental and regression analytical results, the approximate ITZ migration coefficient is 2.83, 1.76 and 1.55 times of the matrix migration coefficient for the ITZ with the assumed thickness of 20, 40 and 50 μm, respectively.

From Eq. (6), the migration coefficient of ITZ ($D_{TZ} = \alpha D_o$) is obtained as:

$$\alpha D_o = \frac{D_{cl}}{(\beta V_f)} - \frac{D_o(1 - V_f)^{3/2}}{(\beta V_f)} + D_o. \quad (8)$$

Based on the experimental and regression analytical results, the relationship between normalized chloride migration coefficient of ITZ ($\alpha = D_{TZ}/D_o$) and the assumed thickness of ITZ is shown in Fig. 6. As $\beta V_f \to \infty$, the volume of ITZ replaces the total volume of matrix paste. The asymptotic value of Eq. (8) when $\beta V_f \to \infty$ is D_o.

4. Conclusions

The chloride migration coefficient of mortar is influenced by the chloride migration coefficient of matrix, volume fraction of aggregate, the migration coefficient of ITZ and the volume fraction of ITZ. In this study, chloride migration coefficient demonstrates that the tortuosity and ITZ effects are about the same in magnitude but opposite in sign. The chloride migration coefficient is influenced by dilution effect more than by tortuosity or ITZ effect. The volume of ITZ depends on the total aggregate surface and the interface thickness. Based on the experimental and regression analytical results, the approximate chloride migration coefficient of ITZ is about 2.83, 1.76 and 1.55 times of the matrix migration coefficient for the ITZ with the thickness of 20, 40 and 50 μm, respectively.

Acknowledgments

The financial support of National Science Council, ROC, under the grants NSC 90-2211-E-019-022 is gratefully appreciated.

References

[1] M. Castellote, C. Andrade, M.C. Alonso, Changes in concrete pore size distribution due to electrochemical chloride migration trials, ACI Mater. J. 96 (3) (1999) 314–319.
[2] H. Saito, S. Nakane, Comparison between diffusion test and electrochemical acceleration test for leaching degradation of cement hydration products, ACI Mater. J. 96 (2) (1999) 208–212.
[3] S.W. Cho, C.C. Yang, R. Huang, Influence of aggregate content on the transport properties of mortar using accelerated chloride migration test, Concr. Sci. Eng. (2000) (accepted).
[4] S.P. Shah, High performance concrete: Past, present and future, in: C.K.Y. Leung, Z. Li, J.T. Ding (Eds.), High Performance Concrete-Workability, Strength and Durability, Hong Kong University of Science and Technology, Hong Kong, 2000, pp. 3–29.

[5] A. Delagrave, J.P. Bigas, J.P. Olivier, J. Marchand, M. Pigeon, Influence of the interfacial zone on the chloride diffusivity of mortars, Adv. Cem. Based Mater. 5 (3–4) (1997) 86–92.
[6] P.C. Aitcin, P.K. Mehta, Effect of coarse aggregate characteristics on mechanical properties of high-strength concrete, ACI Mater. J. 87 (2) (1990) 103–107.
[7] D. Breton, A. Carles-Gibergues, G. Ballivy, J. Grandet, Contribution to the formation mechanism of the transition zone between rock-cement paste, Cem. Concr. Res. 23 (2) (1993) 335–346.
[8] D. Bonen, Calcium hydroxide deposition in the near interfacial zone in plain concrete, J. Am. Ceram. Soc. 77 (1) (1994) 193–196.
[9] K.L. Scrivener, K.M. Nemati, Percolation of pore space in the cement paste/aggregate interfacial zone of concrete, Cem. Concr. Res. 26 (1) (1996) 35–40.
[10] K.L. Scrivener, E.M. Gartner, Microstructure gradients in cement paste around aggregate particles, in: S. Midess, S.P. Shah (Eds.), Bonding in Cementitious Composites, Materials Research Society, Warrendale, 1988, pp. 77–85.
[11] R.J. Detwller, P.J.M. Monteiro, H.R. Wenk, Z. Zhong, Texture of calcium hydroxide near the cement aggregate interface, Cem. Concr. Res. 18 (5) (1988) 823–829.
[12] S. Diamond, S. Mindess, SEM investigations of fracture surfaces using stereo pairs: I. Fracture surfaces of rock and of cement paste, Cem. Concr. Res. 22 (1) (1992) 67–78.
[13] S. Diamond, S. Mindess, SEM investigations of fracture surfaces using stereo pairs: II. Fracture surfaces of rock-cement paste composite specimens, Cem. Concr. Res. 22 (4) (1992) 678–688.
[14] S. Diamond, S. Mindess, SEM investigations of fracture surfaces using stereo pairs: III. Fracture surfaces of mortars, Cem. Concr. Res. 24 (6) (1994) 1140–1152.
[15] K.L. Scrivener, A. Bentur, P.L. Pratt, Quantitative characterization of the transition zone in high strength concretes, Adv. Cem. Res. 1 (4) (1988) 230–237.
[16] T. Sugama, N. Carciello, L.E. Kukacka, G. Gray, Interface between zinc phosphate-deposited steel fibres and cement paste, J. Mater. Sci. 27 (1992) 2863–2872.
[17] P. Raivio, L. Sarvaranta, Microstructure of fiber mortar composites under fire impact effect of polypropylene and polyacrylonitrile fibers, Cem. Concr. Res. 24 (5) (1994) 896–906.
[18] A. Goldman, A. Bentur, Effects of pozzolanic and non-reactive microfillers on the transition zone in high strength concretes, in: J.C. Maso (Ed.), Interfaces in Cementitious Composites, E&FN Spon, London, 1992, pp. 53–61.
[19] J.P. Ollivier, J.C. Maso, B. Bourdette, Interfacial transition zone in concrete, Adv. Cem. Based Mater. 2 (1) (1995) 30–48.
[20] D.N. Winslow, M.D. Cohen, D.P. Bentz, K.A. Snyder, E.J. Garboczi, Percolation and pore structure in mortars and concrete, Cem. Concr. Res. 24 (1) (1994) 25–37.
[21] J.D. Shane, T.O. Mason, H.M. Jennings, E.J. Garboczi, D.P. Bentz, Effect of the interfacial transition zone on the conductivity of Portland cement mortars, J. Am. Ceram. Soc. 83 (5) (2000) 1137–1144.
[22] E.J. Garboczi, D.P. Bentz, Digital simulation of the aggregate–cement paste interfacial zone in concrete, J. Mater. Res. 6 (1) (1991) 196–201.
[23] E.J. Garboczi, Computational materials science of cement-based materials, Mater. Struct. 26 (158) (1993) 191–195.
[24] C.M. Neubauer, H.M. Jennings, E.J. Garboczi, Three-phase model of the elastic and shrinkage properties of mortar, Adv. Cem. Based Mater. 4 (1) (1996) 6–20.
[25] E.J. Garboczi, D.P. Bentz, L.M. Schwartz, Modelling the influence of the interfacial zone on the DC electrical conductivity of mortar, Adv. Cem. Based Mater. 2 (5) (1995) 169–181.
[26] E.J. Garboczi, D.P. Bentz, Multiscale analytical/numerical theory of the diffusivity of concrete, Adv. Cem. Based Mater. 8 (2) (1998) 77–88.
[27] E.J. Garboczi, D.P. Bentz, Analytical formulas for interfacial transition zone properties, Adv. Cem. Based Mater. 6 (3–4) (1997) 99–108.
[28] D.A.G. Bruggeman, Berechnung verschiedener physikalischer Konstanten von heterogenen Substanzen: I. DielektrizitaÈtskonstanten und LeitfaÈhigkeiten der MischkoÈrper aus isotropen Substanzen, Ann. Phys. (Leipzig) 24 (1935) 636–679.
[29] C.C. Yang, S.W. Cho, R. Huang, The relationship between charge passed and the chloride-ion concentration in concrete using steady-state chloride migration test, Cem. Concr. Res. 32 (2) (2002) 45–50.
[30] C. Andrade, Calculation of chloride diffusion coefficients in concrete from ionic migration measurements, Cem. Concr. Res. 23 (3) (1993) 724–742.
[31] D.P. Bentz, E.J. Garboczi, E.S. Lagergren, Multi-scale microstructural modeling of concrete diffusivity: Identification of significant variables, Cem., Concr., Aggregates 20 (1) (1998) 129–139.